Chinese Chemical Letters 35 (2024) 108639

Contents lists available at ScienceDirect

Chinese Chemical Letters

journal homepage: www.elsevier.com/locate/cclet

Enhancement of catalytic activity for hydrogenation of nitroaromatic by anionic metal-organic framework

Qi Wu[1], Anyang Li[1], Ruibo He, Yaxi Wu, Lei Hou, Guoping Yang, Wenyan Zhang*, Yao-Yu Wang

Key Laboratory of Synthetic and Natural Functional Molecule of the Ministry of Education, College of Chemistry & Materials Science, Northwest University, Xi'an 710127, China

ARTICLE INFO

Article history:
Received 27 February 2023
Revised 3 May 2023
Accepted 31 May 2023
Available online 5 June 2023

Keywords:
Anions
Metal-organic frameworks
Catalysis
Electron transfer
Hydrogen production

ABSTRACT

Nitroaromatic hydrogenation catalysis without precious metals remains a longstanding challenge. The rate of electron transfer is the crucial factor affecting hydrogenation catalysis. Herein, an ionic Cd-based metal-organic framework (I-Cd-MOF) exhibiting a unique structure with one-dimensional (1D) opening nanochannels and good electron transfer ability was synthesized for catalyzing hydrogenation of 4-nitrophenol (4-NP). The catalytic activity of the unique I-Cd-MOF without noble metals is detected, which is higher than most reported noble metal catalysts. Remarkably, the reaction rate of I-Cd-MOF (4.28 min^{-1}) is about 47.6 times higher than that of the Cd-based neutral MOF (N-Cd-MOF) with the similar crystalline structure. Liquid chromatograph mass spectrometer (LC-MS) and theoretical results demonstrate that 4-NP and five intermediates are stabilized in the channels of I-Cd-MOF, which increases the possibility of contact with H^* and H_2 generated at the Cd sites. The I-Cd-MOF was extended to other nitroaromatic hydrogenation catalysis, which still displays excellent activity. More importantly, the I-MOF@Filter membrane was successfully constructed for continuous hydrogenation catalytic reactions, which maintains a high catalytic performance after 7 cycles of recycling without washing. This work fills in the application of the I-MOFs in hydrogenation catalytic reactions and provides an effective way for the rapid and green degradation of nitroaromatic compounds.

Nitroaromatic compounds are difficult to degrade in the natural environment, and they have been listed in the Environmental Priority Control Pollutants List of the US Environmental Protection Agency [1–5]. A certain amount of nitroaromatic compounds may cause increased levels of methemoglobin in humans, leading to blue spot disease and even severe neurological damage [6]. Among them, 4-NP is one of the most harmful and representative. The chemical reduction of 4-NP in wastewater not only benefits to environmental protection but also generates high-value products of 4-Aminophenol (4-AP) [7].

In the past decades, for catalyzing the reduction of 4-NP, the H_2 or $NaBH_4$ as reducing agents are employed with precious metal-loaded catalysts (such as Au, Pd, Pt, and Ag) have been reported, showing excellent results [8–10]. Most of them are compounded materials of precious metals and porous materials to reduce the aggregation of precious metal nanoparticles [11–16]. For example, a Pd/O-CNT nanocomposite catalyst with good catalytic performance (K_{app} value is 1.07 min^{-1}) was reported [17]. In the catalyst, the crucial electron transfer contribution of CNT for capturing the electrons in the catalysis reaction was demonstrated. However, continuous nitroaromatic hydrogenation catalysis without noble metals at room temperature remains a great challenge.

MOF is a periodic organic-inorganic hybrid material which is self-assembled by metal ions (or metal clusters) and organic ligands through coordination bonds [18]. Considering their high porosity and chemical tunability, these materials have been intensively investigated in applications such as adsorption [19–21] and catalysis [22–25]. Nevertheless, a part of MOF's framework retains residual charge during self-assembly to form ionic MOFs (I-MOFs), which gives superior performance compared to neutral MOFs (N-MOFs) [26]. Recently, the research on I-MOFs in adsorption [27–29], drug delivery [30], sensing [31–33], and battery diaphragm [34–37] has gradually increased, which is due to the unique pore channel of I-MOF and electrostatic interaction between the ionic framework and the guest of I-MOF [38]. However, the ability of I-MOF to accelerate electron transfer is not yet well developed, which is a crucial factor for catalytic activity. Therefore, I-MOFs

* Corresponding author.
E-mail address: zhangwy@nwu.edu.cn (W. Zhang).
[1] These authors contributed equally to this work.

https://doi.org/10.1016/j.cclet.2023.108639
1001-8417/

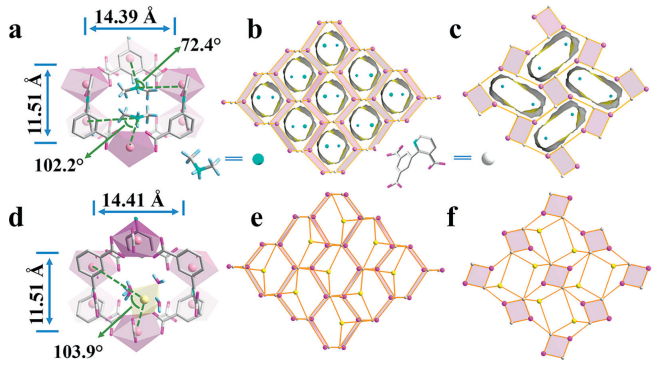

Fig. 1. (a) The pore channel of I-Cd-MOF along the *c* axis. The simplified model of the pore channel of I-Cd-MOF (b) along the *c* axis and (c) *a* axis, respectively. (d) The pore channel of N-Cd-MOF along the *a* axis. The simplified model of the pore channel of N-Cd-MOF (e) along the *a* axis and (f) *c* axis, respectively. Pink: seven-coordinated Cd atom; Yellow: six-coordinated Cd atom; Green: $(CH_3)_2NH_2^+$; White: H_3L ligand; Red: oxygen atom; Blue: hydrogen atom.

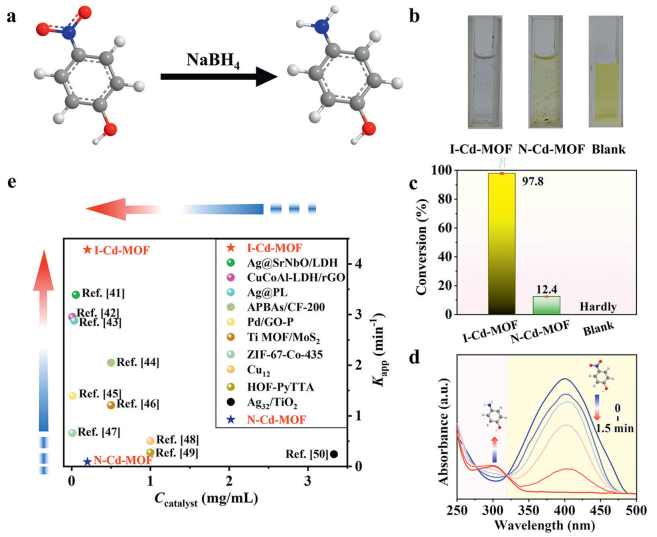

Fig. 2. (a) The reaction formula of the catalytic reaction (2 mL of 0.2 mol/L $NaBH_4$, 0.2 mL of 1.00 mmol/L 4-NP, and 0.1 mL of 0.2 mg/mL catalyst). (b) The pictures of the reaction of different catalysts. (c) Conversion of I-Cd-MOF, N-Cd-MOF, and blank sample within 1.5 min. (d) UV–vis absorption spectra of I-Cd-MOF for catalytic reduction of 4-NP. (e) Comparison of catalyst reaction rate and the amount of catalyst.

are expected to replace precious metals in catalytic hydrogenation. Herein, an I-Cd- MOF, $\{[(CH_3)_2NH_2^+][Cd(L)]\}_n$, with 1D opening channels and high electron transfer ability was constructed for catalyzing the chemical reduction of 4-NP and investigating the reaction mechanism. The N-Cd-MOF, $[Cd_3(L)_2(H_2O)_4]_n$, with the similar crystalline structure was synthesized as a contrast sample. Compared with the N-Cd-MOF, I-Cd-MOF delivered a higher electron transfer rate and 3.4 times higher hydrogen production. The I-Cd-MOF showed a superior catalytic conversion ratio of 97.8% and durability of 5 times catalysis cycles for the reduction of 4-NP. In addition, I-Cd-MOF was constructed with nylon as an I-MOF@Filter membrane for rapid continuous catalytic hydrogenation of 4-NP at room temperature.

I-Cd-MOF and N-Cd-MOF were synthesized from (2-(3,5-dicarboxyphenyl) nicotinic acid) (H_3L) ligand and Cd(II) (Fig. S1 in Supporting information). I-Cd-MOF crystallizes in the monoclinic space group $P2_1/c$. As shown in Fig. 1a, a Cd(II) ion is coordinated by four differently oriented L^{3-} ligands to be a 3D framework. In the *c* axis, the 1D nanochannel with the size of 11.51 × 14.39 Å is formed. These nanochannels provide good mass transfer routes for the catalytic reactions. The molecule-accessible void of 38.4%, and filled with 9.2% of $(CH_3)_2NH_2^+$ guest ions obtained by Thermogravimetric analyses (TGA) (Fig. S4 in Supporting information). These $(CH_3)_2NH_2^+$ were obtained by hydrolysis and decarbonylation of DMF in the presence of water, and can be used as templates to lead to the formation of anionic frameworks. The 3D framework of I-Cd-MOF is simplified as (4,4)-connected 4-c topology with a point symbol of $\{4^2{\cdot}6^3{\cdot}8\}$ (Figs. 1b and c). N-Cd-MOF has the similar crystalline structure and the similar channel size to I-Cd-MOF (Fig. 1d). However, the channel of N-Cd-MOF is occupied by a six-coordinated Cd_3 instead of $(CH_3)_2NH_2^+$, and the molecule-accessible void of N-Cd-MOF is 20.8% after desolventization calculated by PLATON (Figs. 1e and f). Powder X-ray diffraction (PXRD) data and TGA (performed under an N_2 atmosphere) data indicate that I-Cd-MOF and N-Cd-MOF have good phase purity, good chemical stability, and good thermal stability (Figs. S2-S4 in Supporting information).

Motivated by the larger porosity and better stability, we proceeded to investigate the catalytic behaviors of two MOFs. The catalysis performance for two MOFs toward the reaction of 4-NP to 4-AP was evaluated (Figs. 2a and b). As shown in Fig. 2c, I-Cd-MOF only takes 1.5 mins to convert 4-NP to 4-AP with a conversion ratio of 97.8%. As a comparison, the 12.4% conversion ratio for N-Cd-MOF at 1.5 mins and only 0.15% for the blank sample are observed. In this catalytic process, the reaction of 4-NP follows first-order kinetics [39]. The first-order rate constant K_{app} for 4-NP is calculated as: $-K_{app}\,t = \ln(C_t/C_0) = \ln(A_t/A_0)$, where A_t and A_0 denote the absorbance at the given time and the initial time [40]. As shown in Fig. 2d, Fig. S6 (Supporting information), the K_{app} value of I-Cd-MOF is 4.28 min^{-1}, which is about 47.6 times higher than that of N-Cd-MOF (0.09 min^{-1}). According to the literature, I-Cd-MOF displays superior catalytic activity and durability, which is even higher than most reported noble metal catalysts (Fig. 2e, Figs. S8 and S9 in Supporting information) [41–50].

The two MOFs with similar structures show significantly different activities in the hydrogenation reaction, which attracts our attention to explore the potential catalytic mechanism of anionic skeletons. The rate of electron transfer is the crucial factor for determining the reduction kinetics of 4-NP, which could be evaluated by electrochemical impedance spectroscopy (EIS). The Nyquist plots in Fig. 3a indicate that about 1/2 times smaller charge transfer resistance (R_{ct}) of I-Cd-MOF (64.02 Ω) than that of N-Cd-MOF (116.07 Ω). The faster electron transfer rate contributes to the fast catalysis of 4-NP [51,52]. Moreover, the electrochemical response tests on catalysts, BH_4^-, and 4-NP by *I-t* curves are investigated for evaluating electron transfer abilities [53]. The current responses for I-Cd-MOF showed 2.7 times ($NaBH_4$), 3.1 times (4-NP) higher than those of N-Cd-MOF. For I-Cd-MOF, the current responses of $NaBH_4$ and 4-NP added separately are 5 times that of mixed before added. Indicating that I-Cd-MOF acts as a bridge for electron transfer, the electron transfer efficiency between I-Cd- MOF and the reactants is higher than that of N-Cd-MOF (Fig. 3b). X-ray photoelectron spectroscopy (XPS) of two MOFs were studied in Fig. 3c and Fig. S9. Among them, Cd $3d_{5/2}$ of I-Cd-MOF decreases by 0.5 eV more than that of N-Cd-MOF (0.2 eV, as shown in Fig. S10 in Supporting information). Indicating that I-Cd-MOF is easy to accept electrons to generate Cd-H for efficient catalysis [54]. The importance of I-Cd-MOF as an electron transport bridge between $NaBH_4$ and 4-NP was demonstrated.

Furthermore, in Fig. 3d, two oxidation peaks at −0.8∼−0.6 V and −0.4∼−0.3 V are observed in the positive scan, representing the species of H_2 (hydrogen), and H^* (absorbed hydrogen), respectively [55]. In Fig. S11 (Supporting information), the area of the enclosed curve of the I-Cd-MOF is larger than that of N-Cd-MOF, denoting that I-Cd-MOF is more active than N-Cd-MOF. The intense

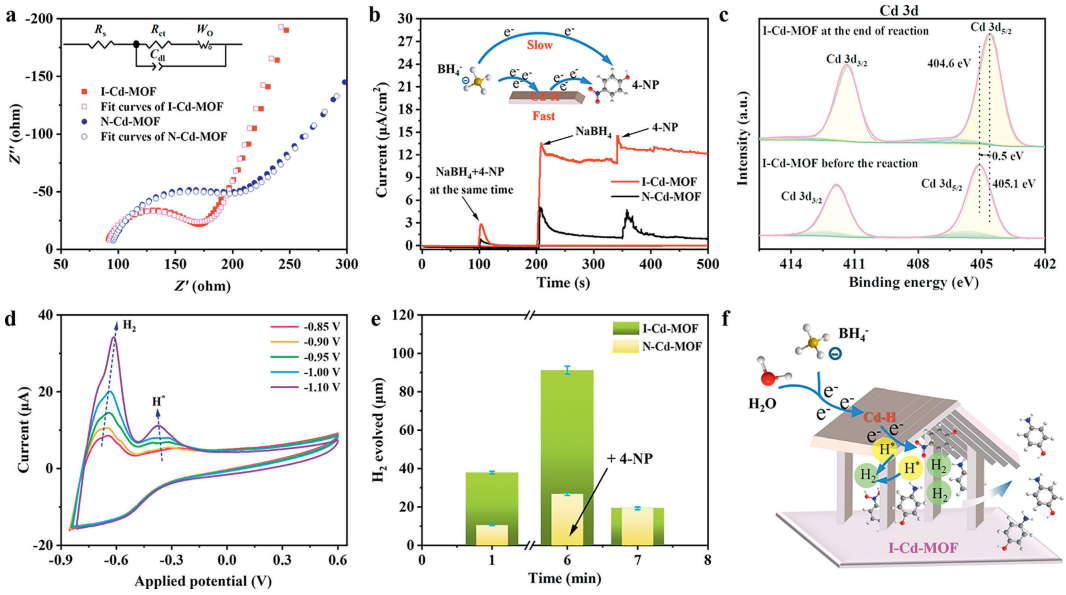

Fig. 3. (a) EIS Nyquist plots of I-Cd-MOF and N-Cd-MOF, respectively. (b) *I-t* curves (at 0 V *vs.* open circuit potential) of I-Cd-MOF and N-Cd-MOF (Inset: The scheme of I-Cd-MOF as the electron transport bridge). (c) The Cd 3d XPS of I-Cd-MOF before the reaction and at the end of the reaction. (d) CV curves of I-Cd-MOF. (e) Comparison of hydrogen production of I-Cd-MOF and N-Cd-MOF. (f) The mechanism of catalytic reaction.

peaks of H_2 for I-Cd-MOF are in accordance with the strong leaking of bubbles during the 4-NP catalytic reaction. Meanwhile, the catalyst after the reaction turns from colorless to dark gray, verifying that the hydrogen spillover occurs on the catalyst [56]. Moreover, the hydrogen production of I-Cd-MOF used in the catalytic reaction is tested. As shown in Fig. 3e and Fig. S12 (Supporting information), the hydrogen production of I-Cd-MOF catalyzed in 6 mins is 3.4 times higher than that of N-Cd-MOF, which is beneficial to further obtain H* species and hydrogenation of polar functional groups (such as nitro) [57,58]. After collecting the sample at the 6th minute, 4-NP was added to the system. The amount of hydrogen in the system decreased in one minute immediately, surprisingly when I-Cd-MOF is used as the catalyst, the hydrogen consumption is almost 9.7 times that of N-Cd-MOF. Those also demonstrate the better catalytic activity of I-Cd-MOF in the reaction. For exploring the catalytic universality of I-Cd-MOF towards nitroaromatic hydrogenation reactions. The reactant nitroaromatics were extended to 2,4-dinitrophenol (DNP), 4-nitroaniline (PNA), 3-fluoro-4-nitrophenol (FNP), dodecyl 2-nitrophenyl ether (ETH 217), *etc.*, all of which display excellent catalytic activity (Fig. S13 in Supporting information). The conversion ratios of 97.2%, >99.0%, 94.1%, and >99.0% were observed, respectively.

Trapping reaction intermediates catalysts is difficult, especially when doing so simultaneously [59–62]. Interestingly, owing to the intense electrostatic interaction of ionic 3D skeletons for I-Cd-MOF the effective trapping of reactants and 4-(dihydroxyamino) phenol (**II** *m/z* (141+H^+), *m/z* (141+Na^+)), 4-nitrosophenol (**III** *m/z* 123+H^+), 4-Hydroxyphenol (**IV** *m/z* 125), azobenzene compounds and other intermediates (**V** *m/z* 232, **VI** *m/z* 215) were observed by employing LC-MS (Figs. 4a–c). According to the literature [63,64] and the LC-MS spectra, the reduction pathway is clearly revealed in Fig. 4d: To form Cd-H, the metal active Cd centers in I-Cd-MOF firstly accept H* produced by water and promoted by BH_4^-. Afterwards, the electrons of Cd-H are transferred to 4-NP, which promotes the reaction process through the **II, III, IV, V** and **VI** in turn to form 4-AP.

The density functional theory (DFT) was employed for theoretical calculations for studying catalytic reaction mechanisms. The relative stability energy (ΔE) and dihedral angle (ψ) for MOF with different intermediates (MOF@intermediate) are shown in Figs. 4e and f and Fig. S15 (Supporting information). It is expected that ΔE of the I-Cd-MOF@intermediates (47 kcal/mol, 67 kcal/mol, 47 kcal/mol, 42 kcal/mol, and 51 kcal/mol, respectively) are obviously higher than that of the N-Cd-MOF (33 kcal/mol, 59 kcal/mol, 41 kcal/mol, 32 kcal/mol and 43 kcal/mol, respectively). Demonstrating that reactants and intermediates can be more stable in the I-Cd-MOF channel, which increases the possibility of contact with H* and H_2 generated at the Cd sites, thus increasing the reaction rate. Notably, for I-Cd-MOF, the ΔE of MOF@II (67 kcal/mol) is significantly higher than that of other MOF@intermediate (Fig. 4e, Table S5 in Supporting information), which matches the experimental results of LC-MS (Fig. S14 in Supporting information).

Above all, due to its unique anion skeletons, it has a faster electron transfer ability and higher catalytic hydrogen production ability, thus accelerating the reaction rate; In addition, the reactants and intermediates can be stabilized in the anionic skeleton pores, increasing their accessibility to H* and H_2, which is produced by the anionic skeleton's Cd metals [65]. The synergistic action of the anionic skeleton and the Cd active sites greatly improved the catalytic ability of I-Cd-MOF, making it suitable as a catalyst for the hydrogenation reduction of 4-NP (Fig. 3f).

I-Cd-MOF's superb catalytic performance and durability stimulated us to further investigate the industrial continuous catalysis potentials. The 10 mg I-Cd-MOF crystals were deposited on the nylon filter membrane with the thickness of 60 μm. The I-MOF@Filter membrane was assembled into a subatmospheric pressure suction filtration device for continuous catalytic reaction of 4-NP to 4-AP at room temperature (Fig. 5a). The PXRD results (Fig. 5b) show the maintained good crystallinity of I-Cd-MOF on the filter membrane. To our delight, the continuous catalysis of 4-NP for more than 7 times with a maintains high conversion ratio of 94.4% is observed (Fig. 5c). The PXRD patterns, SEM, and EDS mapping images for recycled I-MOF@Filter membrane display the brilliant crystalline structure, and surficial morphology, indicating the superb durability and cycling ability of such a filter (Figs. 5d and e, S16). Owing to the simple and fast assembly method and excellent catalytic performance, the I-MOF@Filter membrane shows promising commercial values.

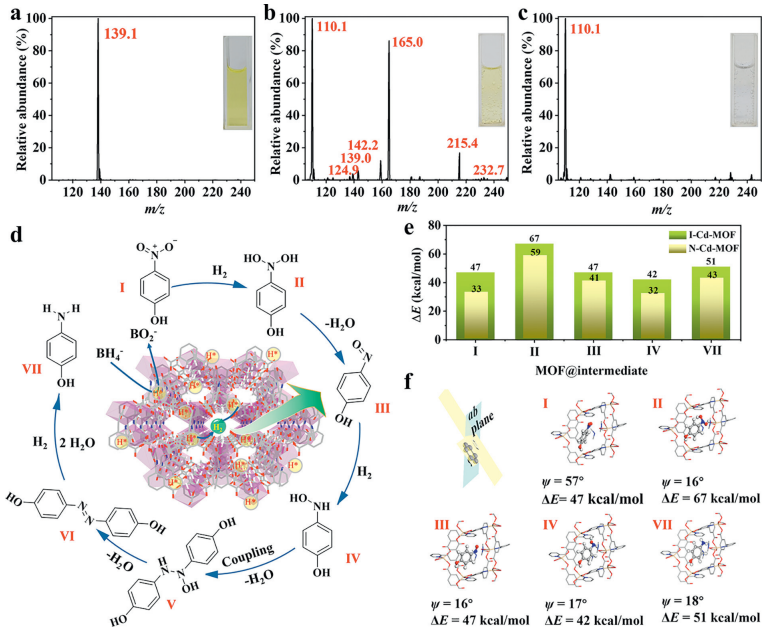

Fig. 4. The LC-MS spectra of I-Cd-MOF used for the catalytic reaction, (a) before, (b) at 30 s, and (c) after the reaction, respectively. (d) The pathway of catalytic hydrogenation of 4-NP to 4-AP by I-Cd-MOF. (e) Stability energy (ΔE) of different MOF@intermediates. (f) Stability energy (ΔE) and dihedral angle (ψ) of different I-Cd-MOF@intermediates.

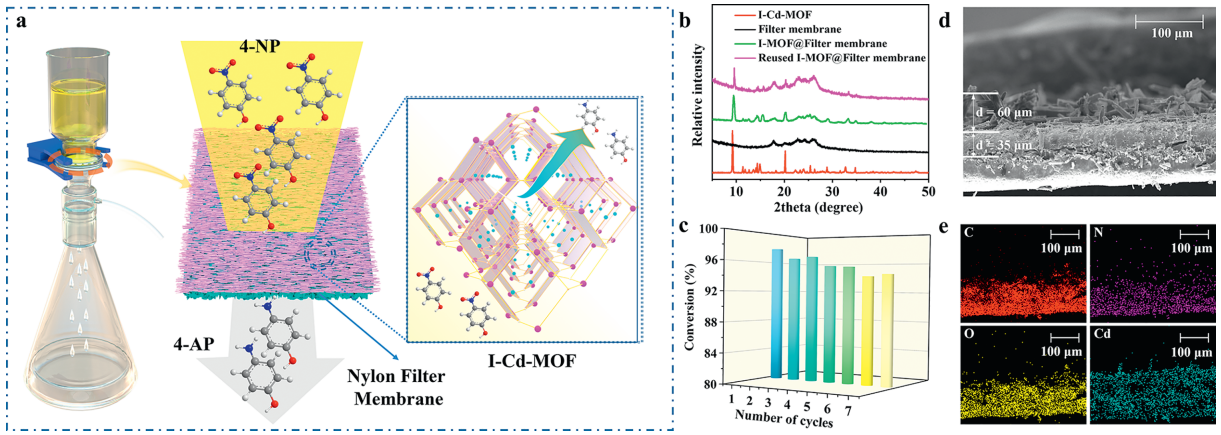

Fig. 5. (a) The scheme of the experimental platform integrating catalytic degradation and filtration separation. (b) PXRD patterns of I-Cd-MOF and I-MOF@Filter membrane before and after reaction. (c) The conversion of the I-MOF@Filter membrane after seven times of reuse. (d) SEM image of I-MOF@Filter membrane. (e) Elemental mapping of I-MOF@Filter membrane.

In summary, a unique nanostructured anionic framework I-Cd-MOF was synthesized and further assembled into the nylon filter membrane for continuous catalysis nitroaromatic hydrogenation reaction. I-Cd-MOF has open 1D nanochannels and $(CH_3)_2NH_2^+$ balanced framework charge, which brings remarkable electron transfer capacity and mass transfer capability. The high conversion ratio of 97.8% based on 4-NP with high stability and recycling ability is observed. The reactant substrate was further extended to other nitroaromatics compounds, showing high-performance catalysis universality. More importantly, the five reaction intermediates for this nitroaromatic hydrogenation reaction are successfully trapped in the pores of the I-Cd-MOF, which greatly benefits revealing the reaction process and plays a dominant role in boosting the reaction kinetics. The I-Cd-MOF not only exhibits a brilliant structural design strategy of crystalline I-MOF catalyst but also showed promising industrial continuous catalysis application potentials. This work fills in the application of the I-MOF in hydrogenation catalytic reaction, highlights the role of the anionic skeletons in catalytic hydrogenation activity, and provides an effective way for the functional development of I-MOF.

Declaration of competing interest

The authors declare that they have no known competing financial interests or personal relationships that could have appeared to influence the work reported in this paper.

Acknowledgments

We are grateful for the financial support provided by the NSFC (No. 21531007), the Shaanxi Provincial Natural Science Basic Research Program (No. 2019JM-590), the Shaanxi Science and Technology Department (Nos. 2022GY-384, 2022JBGS2–07, 2021LLRH-05–21, 2022QFY06–06).

Supplementary materials

Supplementary material associated with this article can be found, in the online version, at doi:10.1016/j.cclet.2023.108639.

References

[1] N. Xu, Q. Zhang, B. Hou, et al., Inorg. Chem. 57 (2018) 13330–13340.
[2] M.C. He, Y. Sun, X.R. Li, et al., Chemosphere 65 (2006) 365–374.
[3] K.S. Ju, R.E. Parales, Microbiol. Mol. Biol. Rev. 74 (2010) 250–272.
[4] D.V. Patil, R.P.B. Somayajulu, G.P. Dangi, et al., Ind. Eng. Chem. Res. 18 (2011) 10516–10524.
[5] L. Xie, D. Liu, H. Huang, et al., Chem. Eng. J. 246 (2014) 142–149.
[6] M. Bilal, A.R. Bagheri, P. Bhatt, S.H. Chen, J. Environ. Manag. 291 (2021) 112685.
[7] G.Q. Niu, C. Si, J.C. Jiao, et al., J. Alloys Compd. 830 (2020) 154696.
[8] Y. Zhang, X. Qu, B. Yan, J. Mater. Chem. C 9 (2021) 3440–3446.
[9] M. Zhao, K. Yuan, Y. Wang, et al., Nature 539 (2016) 76–80.
[10] R.K. Dharman, B.M. Francis, J.S. Ponraj, et al., J. Mater. Res. Technol. 17 (2022) 1760–1769.
[11] X.Q. Xie, Z.J. Wu, N. Zhang, Chin. Chem. Lett. 31 (2020) 1014–1017.
[12] L.Y. Li, Y.X. Li, L. Jiao, et al., J. Am. Chem. Soc. 144 (2022) 17075–17085.
[13] G.F. Liu, X.X. Qiao, Y.L. Cai, et al., ACS Appl. Nano Mater. 3 (2020) 11426–11433.
[14] H. Hu, C.L. Song, D. Wang, et al., Chin. Chem. Lett. 34 (2023) 107770.
[15] A.A. Kassem, H.N. Abdelhamid, D.M. Fouad, et al., Int. J. Hydrog. Energy 44 (2019) 31230–31238.
[16] J.J. Li, X.D. Sun, S. Subhan, et al., Chem. Eng. J. 446 (2022) 137314.
[17] J. Audevard, A. Benyounes, R.C. Contreras, et al., ChemCatChem 14 (2022) e202101783.
[18] M.A. Ghasemzadeh, B. Mirhosseini-Eshkevari, M. Tavakoli, et al., Green Chem. 22 (2020) 7265–7300.
[19] X.Y. Ren, C.C. Wang, Y. Li, P. Wang, S.J. Gao, J. Hazard. Mater. 445 (2023) 130552.
[20] L.H. Meng, C. Zhao, T.Y. Wang, H.Y. Chu, C.C. Wang, Sep. Purif. Technol. 313 (2023) 123511.
[21] A.F. Du, H.F. Fu, P. Wang, C.C. Wang, Chemosphere 322 (2023) 138221.
[22] Y.J. Fu, M. Tan, Z.L. Guo, et al., Chem. Eng. J. 452 (2023) 139417.
[23] S.Z. Zheng, H. Du, L.X. Yang, et al., J. Hazard. Mater. 447 (2023) 130849.
[24] X.F. Zhang, C.Y. Yang, P.F. An, et al., Sci. Adv. 8 (2022) eadd5678.
[25] J. Guo, Y.T. Qin, Y.F. Zhu, et al., Chem. Soc. Rev. 50 (2021) 5366–5396.
[26] J.D. Pang, S. Yuan, J.S. Qin, et al., J. Am. Chem. Soc. 141 (2019) 3129–3136.
[27] J. An, N.L. Rosi, J. Am. Chem. Soc. 132 (2010) 5578–5579.
[28] J.T. Li, P.M. Bhatt, J.Y. Li, M. Eddaoudi, Y.L. Liu, Adv. Mater. 32 (2020) 2002563.
[29] S. Sharma, A.V. Desai, B. Joarder, S.K. Ghosh, Angew. Chem. Int. Ed. 59 (2020) 7788–7792.
[30] I. Imaz, M. Rubio-Martínez, L. García-Fernández, et al., Chem. Commun. 46 (2010) 4737–4739.
[31] Y.H. Takashima, V.M. Martínez, S.H. Furukawa, et al., Nat. Commun. 2 (2011) 168.
[32] Y. Wang, B.Y. Li, J.J. Zhu, et al., Angew. Chem. Int. Ed. 61 (2022) e202201789.
[33] A.V.D Joarder, P. Samanta, et al., Chem. Eur. J. 21 (2015) 965–969.
[34] H. Gao, Y.B. He, J.J. Hou, et al., ACS Appl. Mater. Interfaces 12 (2020) 41605–41612.
[35] H. Gao, Y.X. Wang, Y.B. He, et al., Inorg. Chem. Front. 9 (2022) 2997–3002.
[36] Y.H. Han, Y. Ye, C. Tian, et al., J. Mater. Chem. A 4 (2016) 18742–18746.
[37] S.S. Nagarkar, S.M. Unni, A. Sharma, et al., Angew. Chem. Int. Ed. 53 (2014) 2638–2642.
[38] G. Huang, L. Yang, Q. Yin, et al., Angew. Chem. Int. Ed. 59 (2020) 4385–4390.
[39] M.F. Zayed, W.H. Eisa, A.E.M. Hosam, A.M. Abou Zeid, J. Alloys Compd. 835 (2020) 155306.
[40] L.J. Liu, R.F. Chen, W.K. Liu, et al., J. Hazard. Mater. 320 (2016) 96–104.
[41] J.D. Zhou, X.L. Liu, J.J. Huang, et al., Appl. Surf. Sci. 581 (2022) 152425.
[42] D.Y. Feng, Z.J. Wei, Q.L. Wang, et al., ACS Appl. Mater. Interfaces 14 (2022) 24265–24280.
[43] W.Z. Xiao, L.P. Xiao, Y.Q. Yang, et al., J. Environ. Chem. Eng. 10 (2022) 107945.
[44] F. Chen, X.L. Yan, X.Y. Hu, et al., J. Environ. Manag. 314 (2022) 115075.
[45] T.D. Zhang, B. Ouyang, X.L. Zhang, et al., Appl. Surf. Sci. 597 (2022) 153727.
[46] R.K. Dharman, B.M. Francis, J.S. Ponraj, et al., J. Mater. Res. 17 (2022) 1760–1769.
[47] W.F. Du, F.Y. Han, M.W. Zhang, C. Qian, X.F. Yang, Compos. Commun. 25 (2021) 100718.
[48] C.Y. Liu, S.F. Yuan, S. Wang, et al., Nat. Commun. 13 (2022) 2082.
[49] T.R. Lin, Y. Sun, C.S. Tian, et al., Chem. Eng. J. 441 (2022) 136092.
[50] L.Y. Chen, F. Sun, Q.L. Shen, et al., Nano Res. 15 (2022) 8908–8913.
[51] R. Yan, T. Ma, M.H. Cheng, et al., Adv. Mater. 33 (2021) 2008784.
[52] M.Z. Ding, R.Y. Shi, J. Qu, M.M. Tong, Chin. Chem. Lett. 34 (2023) 108248.
[53] C.H. Xu, X.Y. Pan, L.P. Fang, et al., Chem. Eng. J. 360 (2019) 180–189.
[54] M. Zhang, A. Cao, H. Zhang, et al., J. Colloid Interface Sci. 623 (2022) 63–76.
[55] G.C. Yue, Y. Yu, S. Li, et al., Small 19 (2023) 2207918.
[56] F,G. O'Brien Johnson, P.G. Tratnyek, et al., Environ. Sci. Technol. 50 (2016) 9558–9565.
[57] Y.X. He, N. Cheshomi, S.M. Lawson, et al., Chem. Eng. J. 410 (2021) 128326.
[58] S.L. Zhang, L.F. Zhong, Z.L. Xu, et al., Chemosphere 291 (2022) 132871.
[59] M.J. Hülsey, V. Fung, X.D. Hou, J.S. Wu, N. Yan, Angew. Chem. Int. Ed. 61 (2022) e202208237.
[60] P.A. Sermon, G.C. Bond, J. Chem. Soc. Faraday Trans. 1 72 (1976) 730–744.
[61] Z.J. Han, G. Wang, J. Zhang, Z.Y. Tang, Nano Energy 102 (2022) 107615.
[62] J.L. Cai, J.Y. Yang, X. Xie, et al., Energy Environ. Mater. 6 (2023) e12424.
[63] H.U. Blaser, Science 313 (2006) 312–313.
[64] T. Aditya, A. Pal, T. Pal, Chem. Commun. 51 (2015) 9410–9431.
[65] W.R. Cheng, H.B. Zhang, D.Y. Luan, W.X. Lou, Sci. Adv. 7 (2021) eabg2580.